Romanian Reports in Physics, Vol. 68, No. 1, P. 353–361, 2016

ANALYSIS OF LIMESTONES FROM HERITAGE BUILDINGS AS DAMAGE DIAGNOSTICS

A.-A. BALOG[1], N. COBÎRZAN[1], E. MOSONYI[2]

[1] Technical University of Cluj-Napoca, Faculty of Civil Engineering, Baritiu 25, 4, Cluj-Napoca, Romania, E-mail: anca.balog@dst.utcluj.ro; E-mail: nicoleta.cobarzan@ccm.utcluj.ro,
[2] "Babeş-Bolyai" University, Faculty of Biology – Geology, Kogălniceanu 1, 400084, Cluj-Napoca
E-mail: emilia.mosonyi@ubbcluj.ro

Received September 25, 2014

Abstract. The paper presents the mineralogical-petrographical analysis of two limestone samples collected from Piarists Church of Cluj-Napoca city, in order to identify the causes of their decay. The samples have been analysed in thin sections, using the Alizarin Red S pigment, the X-ray diffraction patterns, and binary image analysis method. The results show that limestone samples have different mineralogical composition, rates of solubility and porosity which justify their different behaviour in time for similar environmental conditions.

Key words: limestone, porosity, X-ray deffraction, Alizarin Red S, image analysis.

1. INTRODUCTION

Weathering plays an important role in all the damage or decay mechanisms of building materials, especially in case of natural stones (limestones, sandstones, volcanic tuffs).

The damage processes of the material's are very complex and depend upon the material's nature which is directly proportional to the rock's characteristics (mineralogical composition, mechanical, physical and chemical properties) and the environmental conditions (pH, temperature, relative humidity, atmospheric pressure and pollution, rain, wind).

Damage due to surface erosion, black crust, detachment of thin stone fragments, salt attack and biological films are often found in many heritage buildings, mostly in those made of limestone blocks [1–7].

Limestone and dolomite rock are calcium carbonate rocks and the magnesium content is the mineral that can made the differences between them. The XRD analysis or EPR spectra [8] are important methods which can be used as qualitative and quantitative determination of carbonate mineral phases, especially for dolomite.

In this respect, the paper presents the mineralogical characteristics of few limestone samples collected from an existing heritage building – the Piarists Church from the city of Cluj-Napoca (Fig. 1 a, b, c) in order to diagnostic their damage's causes.

2. MATERIALS AND METHODS

The Piarists Church is the first ecclesiastic Baroque style building elevated in the 18th century and located in the centre of Cluj-Napoca city. Some of the building's elements are made of blocks of limestone originating from the ruins of the former Jesuit convent [9]. The building was rehabilitated in the last 300 years for many times, beginning with 1775 and finishing in 2011.

In order to identify the causes of the differentially decay of masonry units, were collected and used for these investigations, few fragments of limestone affected by erosion, felt from north and north-west facade of the building (Fig. 1 d, e).

Fig. 1 – The Piarists Church from Cluj Napoca: localization of Cluj-Napoca area on Romania map (a); the Piarists Church on the map of the Cluj-Napoca centre (b); North-west facade of the Piarists Church (c); eroded steps in the north-west facade of the building (d); different erosion of limestone from the same cornice at the north facade (e).

To determine the mineralogical content, the limestone samples were analyzed using a diffractometer with Cu-Ka1 radiation, λ = 1,540598 Å and $2^{o}\theta$/min with continuous scanning from 5 to 60^{o} (2θ).

The petrographic features of the studied limestones in thin sections were evidenced using a Jenapol polarising microscope in transmitted light, Alizarin Red S (ARS) stained rock slices, to distinguish diagenetic dolomitisation from stained calcite in limestone [10–11].

The porosity of the samples was established in two different ways: a conventional method based on laboratory tests (water absorption method) [12] and one based on binary image analysis.

The percentage of the isolated pore (the effective porosity) which is not possible to be evaluated in laboratory tests, was established in binary image analysis [13–16].

3. RESULTS AND DISCUSSION

The diffractogram of the sample A (Fig. 2) indicate a quite homogeneous mineralogical composition, a high content of carbonate, with calcite ($CaCO_3$) – 42.5 %, dolomite $CaMg(CO_3)_2$ – 57% and quartz (SiO_2) – 0.4 %. The sample B diffractogram (Fig. 3) shows an heterogeneous character, with carbonate and silicate in high percent, contains calcite ($CaCO_3$) – 23.6%, dolomite $CaMg(CO_3)_2$ – 32.5%, quartz (SiO_2) – 25.1%, mica (muscovite) – 18.85%.

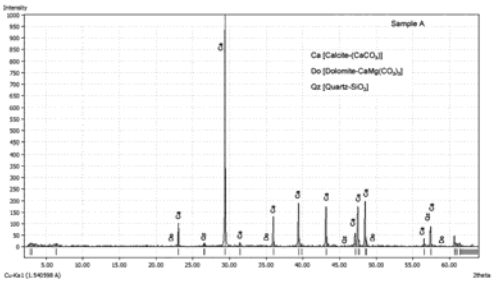

Fig. 2 – X-ray diffraction paterns analysis of sample A (calcite, dolomite and quartz).

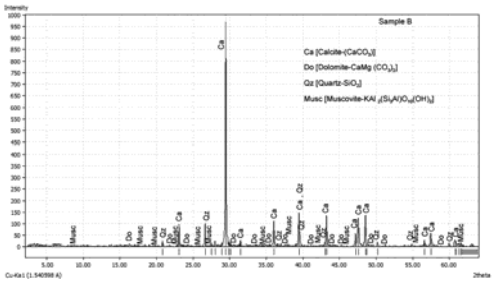

Fig. 3 – X-ray diffraction of sample B (calcite, dolomite, quartz and muscovite).

Based on the three main mineral compounds, dolomite, calcite, non-carbonate, the samples are in the field of Mg-calcite (sample A) and impure Mg-calcite (sample B).

In thin sections, it was established the mineralogical-petrographical content of both samples (sample A – Fig. 4 a, b and B – Fig. 5 a, b).

The sample A contains about 40% coated grains (250–500 microns): ooliths with bioclast cores, pellets, lumps (smaller than 1 mm), Al-Fe-oxide coated sparry carbonate lithoclasts and bioclasts. The mud-supported is a carbonate matrix (about 60%) with rare relict angular or needle-like clasts of 10–20 microns sizes. The opened pores with 50 microns maximum diameter are: elongated intergranular pores, resulted in partially infilling of the 1 mm sized primary pores with mosaic type or fibrous calcite, extensional microfissures partially filled with sparry calcite, and secondary pores, generated in diagenetical dolomitisation process and later partially closed by mosaic type calcite.

Poronecrosis processes observed in thin sections took place by: the primary intergranular pores, infilling with sparry calcite (fenestral structures), solubility and deposition of insoluble clay minerals, iron oxi-hydroxides along the stylolitic surfaces.

a b c

Fig. 4 – Thin section of the sample A: a) oolith (1), lumps (2), bioclasts (3), poronecrosis by sparitic mosaic calcite. Cross polarised light (N+); b) coated grains (1) and mud-supported matrix (2), locally drusic type cement (3), ooids (4), bioclasts (5), cross polarised light (N+); c) Alizarin Red S (ARS) stained surface of rock slice. Dolomite (1) remains uncolored, Calcite (2) is red-orange colored; the scale bar is 1 mm.

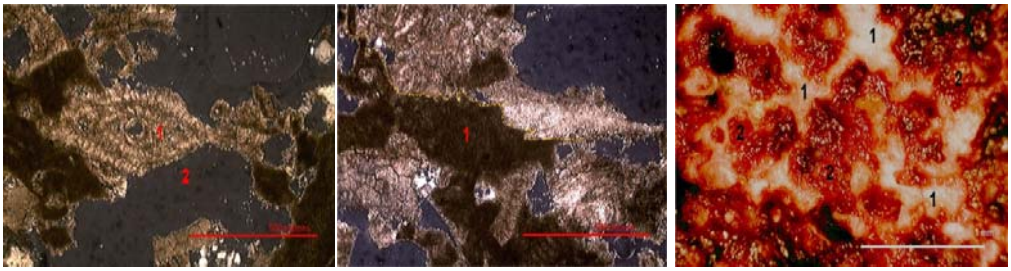

a b c

Fig. 5 – Thin section of sample B: a) cross polarised light. “Bird eyes” microstructure (1) and remnant pore in the centre. The dark grey-colored areas are holes (2) (N+); b) cross polarised light. The cryptocrystalline calcitic bioclasts (Algae (1) boundaries by pressure solution affected (N+)); c. Alizarin Red S stained rock slice. Dolomite (1) remains uncolored, Calcite (2) is red-orange colored; the scale bar is 1 mm.

Sample B (Fig. 5a, b) is a grain-supported limestone consisting in: quartz (200 microns), feldspar, phyllosilicates (micas chlorite), angular limestone intraclasts with narrow sparitic overgrowth zones, bioclasts (mostly algae with cryptocrystalline carbonate mass, associated with foraminifers of 500 microns–1 mm sizes), lithoclasts of quartz sometimes coated with a film of iron oxi-hydroxids (Fig. 4c and Fig. 5c). The matrix of the rock is dominated by micritic carbonate. Diagenetical sparitic carbonate (calcite and dolomite) and fibrous calcite infill „bird eyes" fenestral microstructure and remnant pores.

In thin sections, the holes are maybe due to dolomite removing during thin section preparation.

The both samples were stained with Alizarin Red S pigment to outline the dolomitisation process: calcite is red-orange colored and dolomite remains uncolored (Fig. 4c and Fig. 5c).

The values of the porosity obtained into laboratory are 26.12% for the sample A and 38.3% for the sample B.

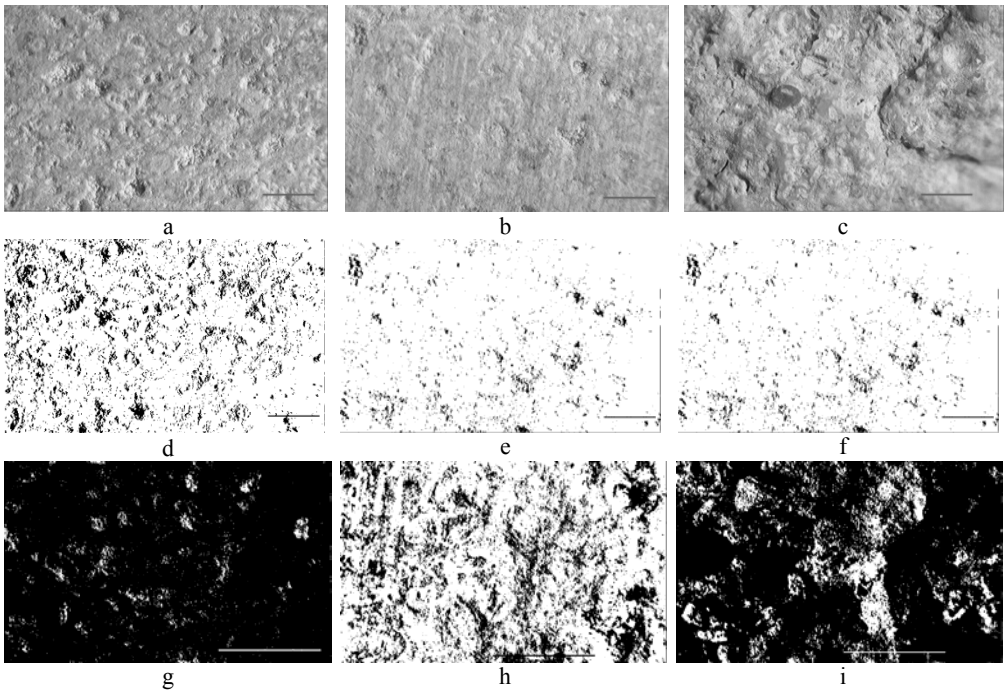

Fig. 6 – Sample A – a, b, c – photo micrographies made at the microscope, on three perpendicular directions; d, e, f – binary images to (×2) magnitude; third line – g, h, i – binary images to (×4) magnitude; the scale bar is 1 mm.

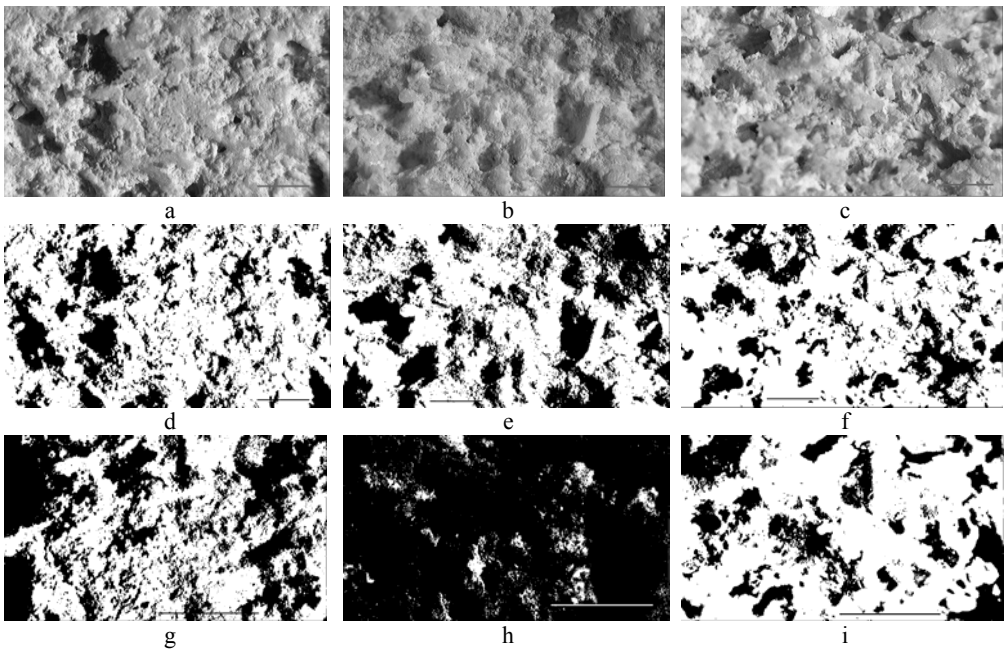

Fig. 7 – Sample B: j, k, l – photo micrographies made at the microscope, on three perpendicular directions; m, n, o – binary images to (×2) magnitude; p, q, r – binary images to (×4) magnitude; the scale bar is 1 mm.

For the binary image analysis the both limestones samples were cut along three perpendicular directions (a 3D expression of the voids/pores was obtained) and micro photographed (Fig. 6 a, b, c and Fig. 7 a, b, c) with a binocular stereo microscope on two magnitudes scale ×2 (Fig. 6 d, e, f and Fig. 7 d, e, f) and ×4 (Fig. 6 g, h, i and Fig. 7 g, h, i).

The images were converted into binary image by identifying two sets of pixels black and white (1 bit/pixel): the black pixels representing the pores (with dimensions between 2 and 50 μ, which is corresponding to capillary pores) and the white pixels the mineral skeleton, bioclasts or clasts.

The opened pores were measured at the polarising microscope, on rock slides, using the micrometre, considering the both magnitude on three directions.

The pores percentage was determined using the ratio between the number of black pixels and the total number of pixels.

The value obtained by the binary image analysis is for sample A, 20.17 %, and for sample B, 33.51%.

An increasing of the concentration of Mg2* (X_{Mg}) in the solid solution of calcite causes the increase of disorder and mineral solubility [17]. The percent of calcite obtained from XRD pattern**,** is 42.5 % and X_{Mg}= 0.14 for sample A, and only 23.6%, respectively X_{Mg}= 0.025 for the sample B. In this respect it results a

more disordered reticular network and a greater calcite dissolution of the sample A comparative with the one of sample B. Due to dedolomitisation processes, the number of calcium ions is increased while that of magnesium ions is decreased, which may create secondary porosity [18–19].

The differences in dissolution of both limestones is due to the content of dolomite (57% in sample A and 32.5% in sample B), increased calcite solubility (sample A) and different content of quartz (0.4% sample A and 25.1% sample B).

The grain sizes influence inversely proportional the dissolution rate [20]. The micrite (< 4 mm grain size) is less soluble than sparite (> 4 mm grain size) and consequently, the allochemical particles such as cortoids, lumps or ooids having sparitic texture will be more easily dissolved than their matrix.

The heterogenous limestone, have different solubility and dilatation/ contraction coefficients of carbonate and non-carbonate extra-clasts (quartz and micas), that give a higher risk of brittle deformation, microfissures and secondary porosity, with pores of distinct geometry (sample B).

Sample B exhibits a higher average porosity determined by decrease of the binding between the grains of quartz and the calcite-dolomite cement, resulting the sand-size quartz grains.

The dissolution of the carbonate is influenced by pH, initial content of carbonate minerals (calcite, dolomite) and concentration of CO_2 from rain water, and the temperature of the environment [21–22].

The calcite dissolution rate increases for $pH < 5$ [23]. On the north-west facade of the building the measured pH of the water on the surface of the limestones, is 6.5 at 17 ^{o} and on the north facade is 6.3 at the same temperature, that means a neutral-lower acid pH, on both part of the building. The difference from this water pH and that of the rain acid value (pH = 5.5) is maybe due to the alkaline caracteristic at the surface of the limestone, given by the carbonate from the limestone, dissolved into the water.

4. CONCLUSION

The heterogeneous limestones (sample B), are more sensitive to weathering decay as the homogeneous one (sample A), because of their mineralogical content.

The case study shows that limestones porosity determined by laboratory tests is higher than that obtain with the binary image analysis. Comparative to the other methods, the binary method used in this paper approaches the porosity by pores dimension and geometry, using two magnitudes scales on three perpendicular directions, to simulate the water transport into the natural stone (by gravity and capillarity).

In this context the binary method is recommended to be used as a complementary method to the conventional ones. A disadvantage of the method is

consisting in the difficulty to identify the very small pores (about microscopic) that can be observed only in SEM (Spectral Electron Microscopy) images.

The mineralogical-petrographical characterization of the building materials can offer complementary informations to the physico-mechanical ones, necessary in design of new buildings or in rehabilitation stage, in order to determine their compatibility and to avoid differential decay.

REFERENCES

1. C. Cardella, D. Benaventeb, J. Rodríguez-Gordilloa, *Weathering of limestone building material by mixed sulfate solutions. Characterization of stone microstructure, reaction products and decay forms*, Materiales Characterisation **59**, *10*, 1371–1385 (2008).
2. O. V. Frank-Kamenetskaya, D. Y. Vlasov, M. S. Zelenskaya, I.V. Knauf, M. A., Timasheva *Decaying of the marble and limestone monuments in the urban environment. Case studies from Saint Petersburg*, *Russia*, Studia Universitatis "Babeş-Bolyai", Geologia **54**, *2*, 17–22 (2009).
3. S. Kramar, A. Mladenović, M. Urosevic, A. Mauko, H. Pristacz, B. Mirtič, *Deterioration of Lesno Brdo limestone on monuments (Ljubljana, Slovenia)*, RMZ – Materials and Geoenvironment **57**, *1*, 53–73 (2010).
4. M. El-Gohary, *Chemical deterioration of Egyptian limestone affected by saline water*, International Journal of Conservation Science **2**, *1*, 17–28 (2011).
5. M.A. El-Gohary, *Investigations on limestone weathering of El-Tuba Minaret El Mehalla, Egypt, A case study*, Mediterranean Archaeology and Archaeometry **10**, *1*, 61–79 (2010).
6. M. Dal, A. D. Öcal, *Limestone in islamic religious architecture: Istanbul and Turkish Thrace*, Metu Journal of the Faculty of Architecture **30**, *1*, 29–44 (2013).
7. M. J. Thornbush, *Photogeomorphological studies of Oxford stone – a review*, Landform Analysis, **22**, 111–116 (2013).
8. D. Covaci, O. G. Duliu, *Preliminary EPR spectra database of natural carbonate of some Romanian quarries*, Romanian Reports in Physics **65**, *2*, 487–494 (2013).
9. M. Toca, *Clujul baroc* (The Baroque Cluj**)**, Editura Dacia, 1983.
10. C. R. B. Jr. Hobbs, *Staining methods for differentiating limestones and dolomites*, Virginia Journal of Science **5**, *4* (1954).
11. B. D. Evamy, *The application of a chemical staining technique to a study of dedolomitisation*, Sedimentology, **2**, 164–170 (1963).
12. STAS 6200/13-80, *Pietre naturale pentru construcţii. Determinarea compactităţii, porozităţii şi a coeficientului de saturaţie* (*Natural stones for building. Determination of compactness, porosity and saturation coefficient*), 1980.
13. O. Rozenbaum, *3-D characterization of weathered building limestones by high resolution synchrotron X-ray Microtomography*, Science of the Total Environment **409**, 1959–1966 (2011).
14. O. Rozenbaum, E. Le Trong, J.L. Rouet, A. Bruand, *2-D image analysis: A complementary tool for characterizing quarry and weathered building limestone*, *Journal of Cultural Heritage*, *8*, 151–159, 2007.
15. M. Buchgraber, M. Al-Dossary, C.M. Ross, A.R. Kovscek, *Creation of a dual-porosity micromodel for pore-level visualization of multiphase flow*, Journal of Petroleum Science and Engineering, 86–87 (2012); 27–38, 2012.
16. M. Freire-Gormaly, H. MacLean, A. Bazyla, *Microct Investigations and pore network reconstructions of limestone and carbonate-based rocks for deep geologic carbon*

sequestration, Proceedings of the 6th International Conference on Energy Sustainability Conference ASME2012, San Diego, California, USA, 2012.
17. M. A. Bertram, F. T. Mackenzie, F. C. Bishop, W. D. Bischoff, *Influence of temperature on stability of magnesian calcite*, American Mineralogist **76**, 1889–1896 (1991).
18. K. Bjørlykke, *Petroleum Geoscience: From Sedimentary Environments to Rock Physics*, Springer, 2010, 508.
19. M. Tadeusz, A. Asuero, *Thermodynamic Modelling of Dolomite Behavior in Aqueous Media*, Journal of Thermodynamics, Volume 2012, Hindawi Publishing Corporation, Article ID723052, 12 pages, 2012.
20. W. D. Bischoff, F. T. Mackenzie, F. C. Bishop, *Stabilities of synthetic magnesian calcites in aqueous solution: comparison with biogenic materials*, Geochimica et Cosmochimica Acta **51**, *6*, 1413–1423 (1987).
21. M. Gautelier, E. H. Oelkers, J., Schott, *An experimental study of dolomite dissolution rates as a function of pH from −0.5 to 5 and temperature from 25 to 80 ^{o}C*, Chemical Geology **157**, *1–2*, 13–26 (1999).
22. E. Garcia, P. Alfonso, E. Tauler, S. Gali, *Surface alteration of dolomite in dedolomitization reaction in alkaline media*, Cement and Concrete Research **33**, *9*, 1449–1456 (2003).
23. O. W. Duckworth, S.T. Martin, *Dissolution rates and pit morphologies of rhombohedral carbonate minerals*, American Mineralogist **89**, 554–563 (2004).